Isoform-Selective Inhibition of the Human UDP-glucuronosyltransferase 2B7 by Isolongifolol Derivatives

Ingo Bichlmaier,[†] Mika Kurkela,[‡] Tanmaya Joshi,[†,§] Antti Siiskonen,[†] Tobias Rüffer,[||] Heinrich Lang,[||] Bohumila Suchanová,[†] Mikko Vahermo,[†] Moshe Finel,[‡] and Jari Yli-Kauhaluoma*[,†]

Division of Pharmaceutical Chemistry, Faculty of Pharmacy, and Drug Discovery and Development Technology Center, University of Helsinki, FI-00014 Helsinki, Finland, Department of Chemistry, Indian Institute of Technology, Kanpur 208016 (UP), India, and Lehrstuhl für Anorganische Chemie, Institut für Chemie, Technische Universität Chemnitz, D-09111 Chemnitz, Germany

Received October 16, 2006

A set of 48 derivatives of the tricyclic sesquiterpenol alcohol isolongifolol was synthesized. The set comprised homochiral and diastereomeric alcohols, amines, chlorohydrins, as well as carboxylic acids, phosphonic acids, and their corresponding esters. The absolute configuration of the epimeric compounds was assigned by 2D NMR experiments [gradient heteronuclear single quantum correlation (gHSQC) and gradient nuclear Overhauser enhancement spectroscopy (gNOESY)] in agreement with crystallographic data. The tricyclic derivatives were assessed as inhibitors of the human UDP-glucuronosyltransferase (UGT) 2B7. The phenyl-substituted secondary alcohol **26b** was the best inhibitor in this series and its competitive inhibition constant was 18 nM. Compound **26b** was not glucuronidated by UGT2B7 and other hepatic UGT enzymes, presumably due to the high steric hindrance exerted by its bulky phenyl substituent. Its inhibitory activity toward 14 other UGT isoforms of subfamily 1A and 2B was determined, and the data indicated that the tricyclic secondary alcohol **26b** was highly selective for UGT2B7 (true selectivity >1000).

Introduction

The UDP-glucuronosyltransferases (UGTs,[a] EC 2.4.1.17) are important enzymes of the human phase II metabolic system. These enzymes catalyze the transfer of α-D-glucuronic acid (GlcA) from UDP-glucuronic acid (UDPGlcA) to lipophilic substrates bearing hydroxy, thiol, amino, sulfonamide, or carboxy groups and even enolate moieties. This conjugation reaction renders lipophilic endobiotics and xenobiotics more water-soluble and stimulates their urinary and biliary excretion, thus preventing their accumulation to harmful levels.[1−3] Eighteen isoforms belonging to either subfamily UGT1 or UGT2 have been identified, seven of which are assumed to play major roles in drug metabolism.[4,5] Perhaps the single most important UGT in drug glucuronidation is UGT2B7, whose activity may account for the transformation of 40% of drugs that are metabolized by UGT isoforms.[5] UGTs are promiscuous enzymes that are commonly described to possess a high degree of flexibility to depict their complex and often overlapping substrate selectivities.[6,7] This feature is assumed to be a defining property of metabolic enzymes such as UGTs, cytochrome P450s, and glutathione S-transferases. These enzymes apparently evolved to possess broad substrate selectivities so that they can detoxify a wide range of harmful compounds.

To date, the crystal structure of the membrane-bound UGTs has not been resolved and the detailed reaction mechanism of the enzymatic glucuronidation reaction is essentially unknown. However, the biotransformation proceeds with inversion of configuration at the anomeric carbon atom of GlcA to afford exclusively β-D-glucuronides. It is therefore assumed that the transfer step is concerted and resembles the bimolecular nucleophilic substitution reaction (S_N2). Two examples for enzyme-catalyzed S_N2 reactions that display the defining transition state with trigonal bipyramidal geometry and penta-coordinate carbon are given by the haloalkane dehalogenase of *Xanthobacter autotrophicus* and S-adenosylmethionine synthetase.[8,9] In contrast, members of the N-ribosyltransferase family were shown to display an S_N1-like mechanism, and several very potent transition-state (TS) analogues for these enzymes were developed.[10,11]

Some inhibitors of the UGT-catalyzed conjugation reaction have been reported, but most of them lack desirable levels of isoform selectivity and potency.[12] Although TS analogues for UGTs were proposed,[13,14] they did not display the high potency that is generally associated with TS mimics.[15] These inhibitors should therefore not be considered as meaningful representations of true TS mimics and could be better described as weak bisubstrate analogues. The lack of potency of these compounds is probably due to the shortfall to address TS-defining features such as bond lengths, bond angles, and electrostatic potential surfaces. In general, true TS analogues are designed on the basis of kinetic isotope effects, computational approaches, and crystallographic analysis, none of which has been conducted for UGT enzymes to date.[16] Therefore and despite various attempts, it has been proven relatively unsuccessful to pursue the design of inhibitors for UGT enzymes by merely attaching a UDP-like entity to a lipophilic moiety.[17,18] Other attempts were driven by random screening of commercially available compounds and one screening approach led to the discovery of

* Corresponding author: phone +358 9 19159170; fax +358 9 19159556; e-mail jari.yli-kauhaluoma@helsinki.fi.

[†] Division of Pharmaceutical Chemistry, Faculty of Pharmacy, University of Helsinki.

[‡] Drug Discovery and Development Technology Center, University of Helsinki.

[§] Indian Institute of Technology.

[||] Technische Universität Chemnitz.

[a] Abbreviations: ^{13}C-δ_{ppm}, chemical shift for ^{13}C in parts per million; $CI_{95\%}$, 95% confidence interval; gCOSY, gradient correlation spectroscopy; gHMBC, gradient heteronuclear multiple bond coherence; gHSQC, gradient heteronuclear single quantum correlation; GlcA, glucuronic acid; gNOESY, gradient nuclear Overhauser enhancement spectroscopy; ^1H-δ_{ppm}, chemical shift for ^1H in parts per million; IBX, 2-iodoxybenzoic acid; IC_{50}, concentration of inhibitor that causes 50% inhibition; J_{HH}, homonuclear coupling constant; K_{ic}, competitive inhibition constant; K_m, Michaelis−Menten constant; *mep*, mixture of epimers; PCC, pyridinium chlorochromate; TS, transition state; UGT, UDP-glucuronosyltransferase.

10.1021/jm061204e CCC: $37.00
Published on Web 05/03/2007

hecogenin as a potentially isoform-selective inhibitor of UGT1A4.[19] Approaches to develop inhibitors for UGT enzymes based on rational design have been rarely conducted.

Isoform-selective and potent inhibitors for UGTs and other metabolic enzymes are valuable tools for pharmacokinetic studies in drug design and development. They facilitate the identification of enzymes that are responsible for drug metabolism and can be applied to testing in human tissue. Furthermore, selective inhibitors can be used to elucidate drug−drug interactions and for the identification of enzyme polymorphism.[7] However, the design of isoform-selective inhibitors for UGTs is difficult because these enzymes display overlapping substrate selectivities and only a small number of selective substrates for some UGT isoforms have been described.[7] This lack of specificity prohibits the derivation of pharmacophores for the design of isoform-selective lead structures. In addition, UGT enzymes generally display low affinities toward their substrates, which renders it difficult to identify structural features that promote high affinity.[5] Yet another major obstacle is that the most common functional groups in organic compounds that promote water solubility, such as hydroxy, amino, thiol, and carboxy groups, serve as nucleophiles in the enzymatic glucuronidation reaction. Hence, the incorporation of such groups bears the risk that the designed inhibitor turns out to be a substrate. The development of potent inhibitors is also challenging because the X-ray crystal structure of any of the UGT isoforms is yet to be resolved. This lack of crystallographic data prevents the design of inhibitors by computational approaches.

The compounds in this study were synthesized from the sesquiterpene (+)-longifolene,[20] and they possess the intricate tricyclo[5.4.0.0^{2,9}]undecane framework, which has attracted the attention of synthetic chemists for decades and for which numerous total syntheses have been reported [the structure of (+)-longifolene is shown in the Supporting Information].[21−23] Furthermore, the terpene has been used for the preparation of dilongifolylborane, an effective chiral hydroborating agent,[24] and chiral longifolylferrocenes have been described.[25] Biosynthesis of the secondary metabolite longifolene was reported and a recent study has investigated the promiscuous enzyme γ-humulene synthase that catalyzes the formation of a prodigious 52 distinct sesquiterpenes, among them longifolene, from the common precursor (*E*,*E*)-farnesyl pyrophosphate.[26,27] The tricyclic sesquiterpene occurs in abundance in the Indian turpentine oil, which is produced commercially from the oleoresin of Himalayan pine, *Pinus longifolia* Roxb. It is used in the perfume industry owing to its woody odor and as a precursor for various other scents.[20] Despite the general interest of organic chemists in the tricyclic terpene, its biological activity was rarely studied, probably due to its low water solubility. In this respect, longifolene was identified as a lipophilic pollutant discharged from a Finnish pulp and paper mill and its potential aquatic toxicity was assessed.[28,29] Its biotransformation was reported and one metabolite, a hydroxyaldehyde, was isolated from rabbit urine.[30] Longifolene was described to be active against Gram-positive bacteria, various fungi, and epimastigotes of *Trypanosoma cruzi*, the causative agent of Chagas disease.[31] Derivatives such as oxime ethers were found to be active against the mosquito *Culex quinquefasciatus*, a vector for the West Nile virus, and oxygenated metabolites were described as inhibitors of butyrylcholinesterase.[32,33]

Our ongoing analysis of stereochemical events during the enzyme-catalyzed glucuronidation reaction has recently shown that diastereomeric tricyclic sesquiterpenoid alcohols display high affinity toward UGT2B7. Furthermore, the rate of the UGT-catalyzed reaction is significantly controlled by stereochemical and steric properties. In contrast, the affinity toward UGT2B7 was not influenced by the stereochemistry of the employed enantiomers and diastereomers.[34−36] These findings provided a rational approach to turn high-affinity substrates into potent inhibitors by addressing stereochemical and steric features to prevent enzymatic glucuronidation. Especially the substrate isolongifolol (**1**) displayed high affinity toward UGT2B7, and therefore, this compound was chosen as the lead compound for this study. In this respect, two sets of isolongifolol derivatives were synthesized. The first set comprised homochiral homologous monofunctional alcohols, carboxylic acids, phosphonic acids, and tertiary amines to identify structural features that are responsible for promoting affinity toward the enzyme (Figure 1). Phosphonic acids were included because it has not been reported to date that phosphono groups are glucuronidated by UGT enzymes. The second set consisted of bifunctional epimeric secondary alcohols bearing various hydrophilic and lipophilic functional groups (Figure 2). The epimers differed from each other only in the configuration in the side chain, designated C(1′) (the numbering of the derivatives is given in the Supporting Information). Therefore, the influence of the spatial arrangement of the hydroxy group and the lipophilic or hydrophilic substituent on the inhibition level could be assessed.

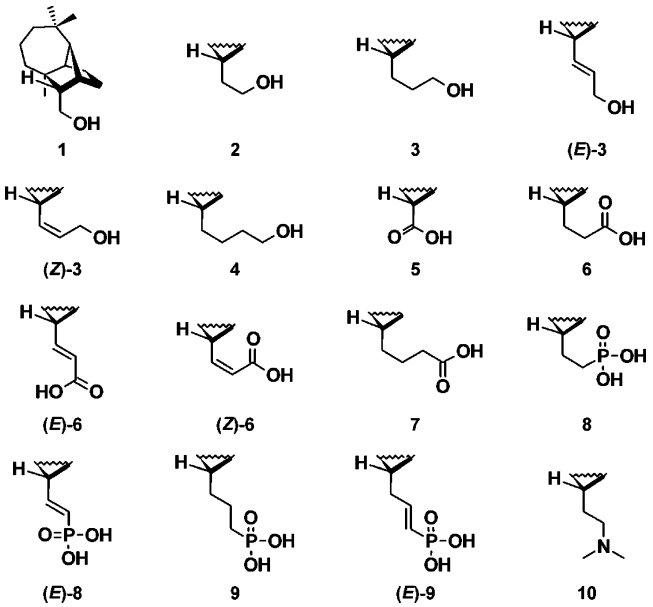

Figure 1. Homochiral isolongifolol derivatives.

Results and Discussion

The syntheses of the isolongifolol derivatives are described in detail in the Supporting Information and only selected synthesis steps are discussed herein. Isolongifolyl aldehyde **32** was an important precursor for the syntheses of the various compounds (compound numbers are given in Schemes 1 and 2 in the Supporting Information). However, the aldehyde **32** was unstable even when stored under inert argon atmosphere at −19 °C, and decomposition was also observed upon storage in vacuo. After storage overnight, decomposition into numerous compounds took place as observed by gas chromatography−mass spectrometry (GC-MS), and the impurities accounted for approximately 20% of the initial pure aldehyde. Therefore, a convenient and fast method for the preparation of **32** was developed by the use of 2-iodoxybenzoic acid (IBX) as the oxidizing agent.[37,38] The terpenoid aldehyde **32** was obtained

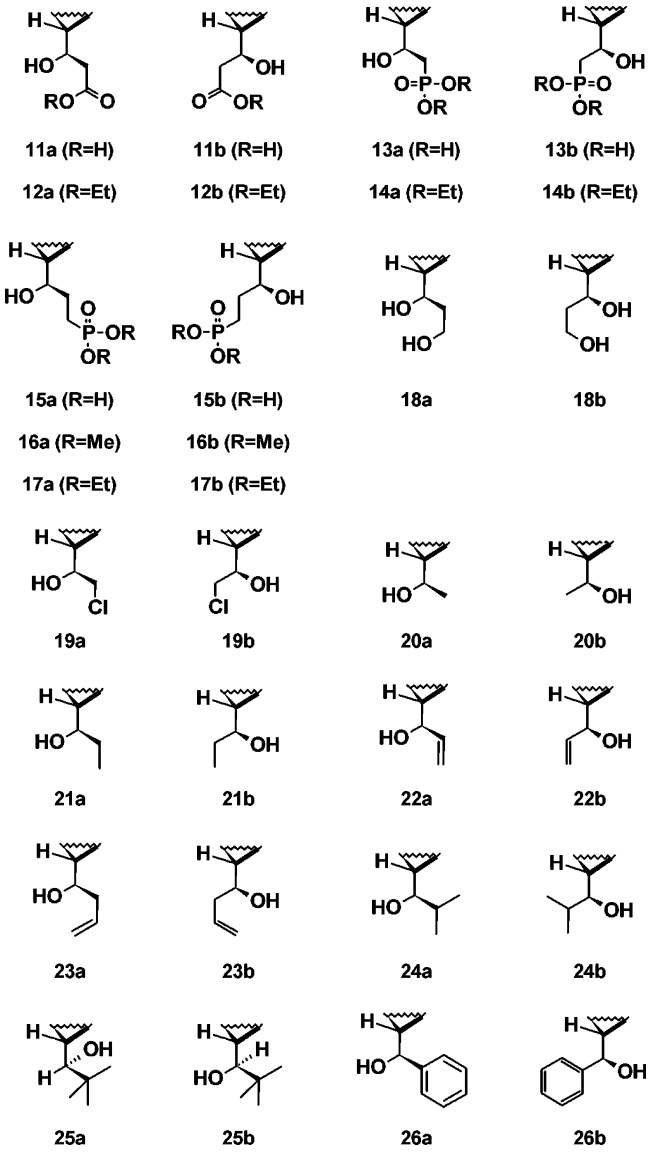

Figure 2. Epimeric isolongifolol derivatives.

in quantitative yield and high purity after aqueous workup without need for further purification. In contrast, when aldehyde **32** was prepared by the use of Dess−Martin reagent or PCC, purification by flash chromatography was necessary due to byproduct formation. Owing to the fast and convenient protocol with IBX, aldehyde **32** was freshly prepared for subsequent synthesis steps. Tertiary amine **10** was synthesized by reductive alkylation from aldehyde **32** by use of triethylsilane and an iridium complex as catalyst.[39] The use of sodium cyanoborohydride and sodium triacetoxyborohydride as reducing agents did not furnish the expected tertiary amine, since the aldehyde **32** was reduced under these conditions and the corresponding alcohol **1** was isolated as the only product.

The oxirane *mep*-**39** was also an important precursor for the preparation of the epimeric bifunctional β- and γ-hydroxyphosphonates and chlorohydrins. Its synthesis was accomplished from aldehyde **32** by the use of diiodomethane and methyllithium.[40] The bifunctional β- and γ-hydroxyphosphonates were prepared by ring opening of the monosubstituted oxirane *mep*-**39** by phosphorus and carbon nucleophiles derived from dialkylphosphites and methanephosphonates, in the presence of boron trifluoride etherate.[41] The monofunctional α,β-unsaturated alkyl phosphonates (*E*)-**35** and (*E*)-**37** were prepared from **32** in a Wittig-type reaction by the use of tetraisopropyl methylenediphosphonate and sodium hydride.[42] The saturated alkyl phosphonates **36** and **38** were synthesized by Pd/C-catalyzed hydrogenation of the olefinic double bonds of (*E*)-**35** and (*E*)-**37**, respectively.[43] The ester bond in alkyl phosphonates was cleaved by use of bromotrimethylsilane followed by hydrolysis of the resulting silyl ester.[42]

The diastereomeric secondary terpenoid alcohols **20a**−**26b** were prepared by Grignard reaction. Pronounced reduction of the aldehyde was observed when the Grignard reagent was employed at <5 equiv. In this case, isolongifolol (**1**) was recovered in yields between 20% and 60%. In contrast, when a solution of the aldehyde was dropped slowly into a solution containing 5 equiv of Grignard reagent, the side reaction was minimized and the desired secondary alcohols were obtained in moderate to good yields. Increasing the amount of Grignard reagent to >5 equiv did not further improve the yields. The bifunctional β-hydroxy esters **12a** and **12b** were synthesized from **32** by titanocene-promoted Reformatsky addition in excellent yields.[44] Subsequent ester hydrolysis afforded the corresponding β-hydroxycarboxylic acids **11a** and **11b**, whereas reduction of the ester group by $LiAlH_4$ gave the corresponding diols **18a** and **18b** in high yields. It should also be mentioned that some solid compounds could be additionally purified by sublimation at relatively low temperatures (23−90 °C; Supporting Information). The chlorohydrin derivatives **19a** and **19b** sublimed slowly at room temperature (23 °C), which was observed when the compounds were dried in vacuo after purification by flash chromatography.

The absolute configuration at C(1′) in the side chain of the epimeric alcohols **12b**, **14a**, **16a**, **17a**, **19b**, **20a**, **21b**, and **22a** was assigned by X-ray crystallography (Supporting Information). However, by conducting 1D and 2D NMR experiments—^{1}H NMR, ^{13}C NMR, gNOESY, gHMBC, gCOSY, and gHSQC—it became evident that the absolute configuration at C(1′) could be conveniently determined by ^{1}H−^{13}C gHSQC correlation analysis, consistent with crystallographic data (Figure 3).[45]

The absolute configuration at C(1′) was assigned by comparing the proton chemical shifts (^{1}H-δ_{ppm}) of the H-atom in position 9, designated C(9)*H*, and that of the H-atoms of the methyl group at position 14, C(14)*H*, of one secondary alcohol to those of its respective epimer. It was observed that when the hydroxy group was pointing toward C(9)*H*, its ^{1}H-δ_{ppm} value was ∼2.30 ppm, whereas the ^{1}H-δ_{ppm} for C(14)*H* was ∼0.90 ppm. Vice versa, when the hydroxy group was in proximity of C(14)*H*, its ^{1}H-δ_{ppm} value was shifted downfield to ∼1.10 ppm, whereas that for C(9)H was ∼2.10 ppm (Figure 3 and Supporting Information). These differences were due to the close proximity of the hydroxy group and the substituent R to either C(9)*H* or C(14)*H* (2.50−2.83 Å in the crystal structures) resulting in different chemical environments and distinct ^{1}H-δ_{ppm} values. The ^{1}H-δ_{ppm} of the endo-positioned C(10)*H* was influenced accordingly, but the differences were in general not as pronounced as those for C(9)*H* and C(14)*H*. The ^{13}C-δ_{ppm} values were not significantly influenced by the spatial arrangement of the substituents, thus facilitating identification of the corresponding carbon atoms in the tricyclic scaffold. The orientation of C(8)*H* to C(1′)*H* was antiperiplanar in the epimeric alcohols (dihedral angle $\phi = 168°-179°$) as can be seen from the crystal structures, and consistently, the coupling constants determined from ^{1}H and gHSQC NMR experiments were ∼10 Hz (Supporting Information). However, the *tert*-butyl-substituted alcohol **25a** displayed significantly smaller $^3J_{HH}$ values of 2.70 Hz in $CDCl_3$ and 2.10 Hz in DMSO-d_6 for C(1′)*H* and C(8)*H*. This small $^3J_{HH}$ indicated a synclinal arrangement of C(8)*H* to

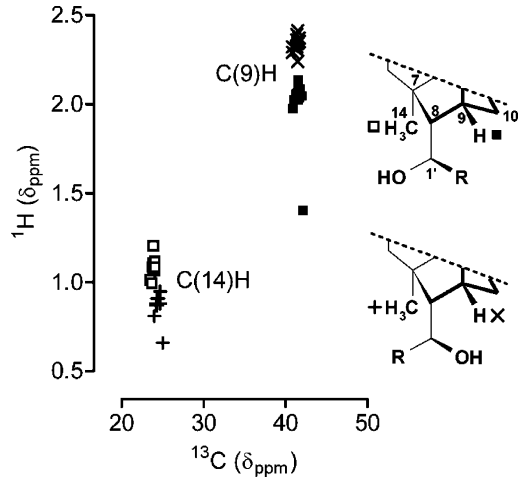

Figure 3. Absolute configuration at C(1′), determined by ^{1}H−^{13}C gHSQC correlation analysis. The graph displays ^{1}H-δ_{ppm} values (ordinate) and ^{13}C-δ_{ppm} values (abscissa) for C(9)H (×, ■) and C(14)H (+, □). Clear differences in the corresponding ^{1}H-δ_{ppm} values enabled the determination of the absolute configuration, in agreement with X-ray crystallographic data. Small variations in the ^{13}C-δ_{ppm} values facilitated the identification of the C-atoms. Deuterated NMR solvents had no significant influence on either ^{13}C-δ_{ppm} or ^{1}H-δ_{ppm} (the graph displays data from NMR experiments with $CDCl_3$, DMSO-d_6, and methanol-d_4). The smallest ^{1}H-δ_{ppm} value for both C(9)H and C(14)H was measured for the phenyl-substituted epimeric alcohols **26a** and **26b**, revealing the highly shielding character of the phenyl group. Data for epimers **25a** and **25b** are not displayed. Detailed gHSQC data along with sample spectra are given in the Supporting Information.

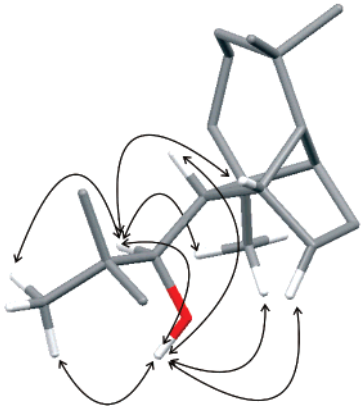

Figure 4. Proposed structure for compound **25a** based on 1D and 2D NMR experiments. NOE correlations for C(1′)O*H* and C(1′)*H* are shown.

C(1′)*H* ($\phi \sim 60°$). Furthermore, gHSQC experiments revealed that the ^{1}H-δ_{ppm} values of C(14)*H* for the diastereomers **25a** and **25b** were 1.00 and 1.07 ppm, respectively, indicating that the OH group was in proximity to C(14)*H* in both epimers. The ^{1}H-δ_{ppm} values for C(9)*H* were small for both stereoisomers (2.03 and 1.90 ppm), indicating that the OH group was distant from C(9)*H* in both diastereomeric alcohols. The most significant difference in the ^{1}H-δ_{ppm} was found for the endo-positioned C(10)*H*, which was significantly smaller for **25b** (1.28 ppm) compared to that for **25a** (2.08 ppm). This very large $\Delta\delta_{ppm}$ of 0.80 ppm indicated that the OH group was close to *endo*-C(10)-*H* in compound **25b** but not in its epimer **25a**. NOE correlations confirmed the proximity of C(1′)O*H* to both C(14)*H* and *endo*-C(10)*H* in **25a**. On the basis of these results, the structure and the absolute configuration at C(1′) for the secondary alcohol **25a** are proposed as displayed in Figure 4 (cf. Supporting Information for a full account). The data showed that the epimer **25a** deviated significantly in its spatial orientation of the hydroxy group from the other diastereomeric derivatives due to the high steric demand of its *tert*-butyl group.

Table 1. Inhibition Levels Exerted by Monofunctional Derivatives

	% inhibition[a]				
compd	100 μM	10 μM	1.0 μM	0.10 μM	IC_{50}^{calc} [b] (μM)
			Primary Alcohols		
1[c]	100	99	92	45*	0.1
2	97	92	68*	15*	0.5
3	100	97	54*	11	0.9
(*E*)-**3**	100	94	56*	15	0.8
(*Z*)-**3**	100	92	60*	14	0.7
4	96	79*	32*	0	3
			Carboxylic Acids		
5	99	90	57*	9	1
6	96	82*	39*	0	2
(*E*)-**6**	98	78*	29*	5	3
(*Z*)-**6**	98	73*	23*	0	3
7	82*	39*	9	0	16
			Phosphonic Acids		
8	92	45*	11	0	12
(*E*)-**8**	89	55*	7	0	8
9	76*	21*	0	0	32
(*E*)-**9**	71*	27*	0	0	41
			Tertiary Amine		
10	91	65*	14*	0	5

[a] Percent inhibition was measured at a constant estriol concentration of 25 μM. The inhibitor concentrations were 0.10, 1.0, 10, and 100 μM. [b] IC_{50}^{calc} = [(100/% inhibition) − 1] × [I]. The value(s) used for the calculation is (are) indicated by the asterisk.[46] [c] The IC_{50} of isolongifolol (**1**) was previously determined (97 nM).[36]

The rotation along the C(1′)−C(8) σ-bond is impaired due to steric hindrance exerted by the C(14)-methyl group on the one side and the *endo*-C(10)*H* on the other side of the tricyclo-[5.4.0.0^{2,9}]undecane scaffold. Therefore, the spatial orientation of the hydroxy group at C(1′) is rather well defined. This highly impaired rotation might be partly responsible for the great differences in the measured ^{1}H-δ_{ppm} values that allowed for the assignment of the absolute configuration at C(1′) (vide supra). It should also be mentioned that the secondary alcohols in which the hydroxy group was pointing toward C(14) possessed higher R_f values than their corresponding epimers and, therefore, eluted from the chromatography column first. In the case of the *tert*-butyl-substituted derivatives **25a** and **25b**, however, the compound **25b** in which the OH group is pointing toward C(14) had a smaller R_f value than **25a** and eluted later from the column.

The affinity toward UGT2B7 was assessed by measuring the reduction of the rate of the enzyme-catalyzed estriol glucuronidation (% inhibition) in the presence of each isolongifolol derivative. The IC_{50} was calculated from this data and was applied to estimate the affinity for each terpenoid derivative (Tables 1 and 2). Estriol was chosen as the reference substrate because this steroid was conveniently detected by fluorescence spectroscopy. In addition, estriol showed simple Michaelis−Menten kinetics without substrate inhibition, and the enzyme assays displayed good reproducibility. The percent inhibition exerted by the substrate isolongifolol (**1**) was applied as a reference to indicate high affinity. The competitive inhibition constant (K_{ic}) of isolongifolol (26 nM) was previously determined in our laboratory.[36]

Table 1 presents the results of the screening assays for the monofunctional derivatives from Figure 1. The IC_{50}^{calc} values varied significantly (0.1−41 μM) and some general trends were observed. The introduction of hydrophilic substituents such as carboxy, phosphono, and amino groups resulted in lower affinities toward UGT2B7. This finding indicated that these groups did not exert significant attractive interactions toward

Table 2. Inhibition Levels Exerted by Bifunctional Derivatives

	% inhibition[a]						% inhibition[a]				
compd	100 μM	10 μM	1.0 μM	0.1 μM	IC_{50}^{calc} [b] (μM)	compd	100 μM	10 μM	1.0 μM	0.1 μM	IC_{50}^{calc} [b] (μM)
Epimeric β- and γ-Hydroxy Acids and Esters											
11a	98	87	53*	12	0.9	**11b**	97	89	51	9	1
12a	100	93	72*	26*	0.4	**12b**	99	94	76*	23*	0.3
13a	81*	36*	8	0	18	**13b**	90	43*	10	0	13
14a	91	49*	8	0	10	**14b**	89	51*	11	0	10
15a	78*	28*	6	0	28	**15b**	83*	36*	7	0	18
16a	99	75*	21*	4	3	**16b**	95	73*	20*	0	4
17a	94	68*	15*	0	5	**17b**	91	70*	27*	0	4
Epimeric Diols and Chlorohydrins											
18a	96	96	82*	38*	0.2	**18b**	99	98	79*	24*	0.3
19a	100	99	88*	36*	0.2	**19b**	97	98	84*	29*	0.2
Epimeric Alkyl, Vinyl and Aryl-Substituted Alcohols											
20a	100	93	66*	13	0.5	**20b**	94	95	59*	11	0.7
21a	100	99	82*	35*	0.2	**21b**	95	97	66*	23*	0.5
22a	95	98	79*	27*	0.3	**22b**	99	94	63*	20*	0.6
23a	100	91	74*	31*	0.4	**23b**	100	100	81*	29*	0.2
24a	99	89	72*	17*	0.4	**24b**	96	96	70*	19*	0.4
25a	99	90	57*	14	0.8	**25b**	94	98	88*	39*	0.2
26a	99	86	53*	24	0.9	**26b**	100	97	94	60*	0.07

[a] Percent inhibition was measured at a constant estriol concentration of 25 μM. The inhibitor concentrations were 0.10, 1.0, 10, and 100 μM. [b] $IC_{50}^{calc} = [(100/\%\ \text{inhibition}) - 1] \times [I]$. The value(s) used for the calculation is (are) indicated by the asterisk.[46]

the binding site of UGT2B7 and therefore did not promote affinity. In this respect, the phosphonic acid derivatives exerted the lowest inhibition levels and (*E*)-**9** displayed the highest IC_{50}^{calc} of 41 μM. Also, elongation of the side chain resulted in lower affinity for both alcoholic and acidic derivatives. This stemmed presumably from the higher flexibility of the longer side chain, leading to an increased entropy cost during formation of the enzyme−inhibitor complex. Accordingly, alcohol **4** and carboxylic acid **7** displayed the highest IC_{50}^{calc} values within the sets of homologous alcohols and carboxylic acids, respectively. Introduction of olefinic double bonds and the resulting geometric isomerism had no significant influence on the affinity because the saturated derivatives **3**, **6**, **8**, and **9** displayed affinities that were comparable to those of their corresponding unsaturated analogues (*E*)-**3**, (*Z*)-**3**, (*E*)-**6**, (*Z*)-**6**, (*E*)-**8**, and (*E*)-**9**. On the basis of these results, it was concluded that there were no attractive interactions between carboxy, phosphono, and amino groups to the binding site of UGT2B7. The substrate isolongifolol was the best inhibitor within the set of monofunctional derivatives. Therefore, it was anticipated that the OH group at C(1′) promoted affinity toward the enzyme.

To test whether the spatial orientation of the OH group at C(1′) is crucial for high affinity, various compounds were synthesized in which this nucleophilic group was retained (Figure 2). The introduction of a second substituent to the diastereotopic C(1′) in isolongifolol (**1**) resulted in two stereoisomers, which were related as epimers. The results of the affinity assays for the epimeric derivatives are displayed in Table 2. The β-hydroxycarboxylic acids, as well as the β- and γ-hydroxyphosphonic acids, displayed the lowest affinities toward UGT2B7. Furthermore, the IC_{50}^{calc} values of these epimeric β- and γ-hydroxy acids **11a**, **11b**, **13a**, **13b**, **15a**, and **15b** were highly similar to those of the respective monofunctional derivatives. This indicated that the hydroxy group had no significant influence on the inhibition level. Hydroxy esters **12a**, **12b**, **14a**, **14b**, **16a**, **16b**, **17a**, and **17b** displayed 1.3−9.3-fold higher affinities toward the enzyme than their respective free acids. This might indicate that lipophilic interactions toward the binding site are favored in agreement with the results for the monofunctional derivatives. In this respect, carboxylic acid esters **12a** and **12b** displayed smaller IC_{50}^{calc} values than the phosphonic acid esters. Also, diols **18a** and **18b**, as well as chlorohydrins **19a** and **19b**, exerted high inhibition levels. The alkyl, vinyl and aryl-substituted derivatives **20a**−**26b** displayed in general high affinities as indicated by IC_{50}^{calc} values below 1 μM. Therefore, it was concluded that lipophilic substituents promote affinity toward UGT2B7. It is noteworthy that the epimers of all compounds displayed highly similar IC_{50}^{calc} values and it was concluded that the spatial arrangement of the hydroxy group had no effect on the inhibition level.

The best inhibitor was **26b**, which displayed a slightly lower IC_{50}^{calc} than isolongifolol (**1**). This indicated that the phenyl group did not significantly contribute to the affinity toward the enzyme. It was therefore concluded that the high affinity stemmed predominantly from hydrophobic interactions between the tricyclic hydrocarbon scaffold and the binding site of the enzyme. However, UGT2B7 was able to accommodate even the bulky phenyl group without loss of affinity. Accordingly, derivatives **25a** and **25b** bearing the sterically demanding *tert*-butyl group also exerted high affinity levels. In this respect, the deviant spatial orientation of the hydroxy group in secondary alcohol **25a** did not result in lower affinity toward the enzyme.

Inhibition of the UGT2B7-catalyzed glucuronidation reaction exerted by compound **26b** was assessed by measuring its IC_{50} value to confirm the apparent high affinity as indicated by the screening assays. This analysis showed that the phenyl-substituted derivative was a potent inhibitor of the UGT2B7-catalyzed estriol glucuronidation as expressed by its low IC_{50} value of 54 nM (standard deviation = 3.9, $n = 18$; $CI_{95\%}$ = 49.2−58.7 nM), which was in good agreement with the IC_{50}^{calc} determined from the screening assays (70 nM). Due to its high affinity, the reversibility of inhibition was measured to determine whether or not the compound was a tight-binding, slowly reversible inhibitor. The reversibility of inhibition was assessed according to standard procedures by measuring the recovery of enzymatic activity after a rapid and large dilution (Supporting Information). The data showed that the sesquiterpenoid alcohol **26b** was a rapidly reversible inhibitor, and standard assays using initial rate measurements could be used for further kinetic studies.

The mode of inhibition—either competitive, uncompetitive, noncompetitive, or mixed-type—was determined by measuring the effects of the $[S]/K_m$ ratio of estriol on the apparent IC_{50} values of the terpenoid alcohol **26b**.[46] As can be seen from

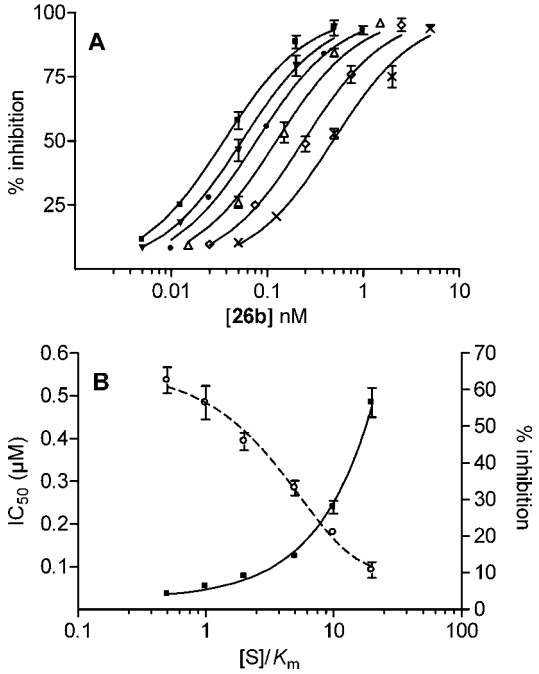

Figure 5. Determination of the mode of inhibition by measuring the effect of [S]/K_m ratio on IC_{50}. (A) Data for each IC_{50} determination;(B) IC_{50} values for **26b** as a function of the [S]/K_m ratio of the reference substrate estriol ($r^2 = 0.987$, left ordinate). (---) Results of the control assays (% inhibition) employing isolongifolol (**1**) at a fixed concentration of 0.10 μM at each [S]/K_m ratio (right ordinate). The mean values and the standard deviations are displayed (panel A, $n = 3$; panel B, $n = 15$ for IC_{50} values, $n = 3$ for control assays). [S]/K_m ratios are plotted on a logarithmic scale for clarity. Compound **26b** displayed the expected behavior for a competitive inhibitor.

Figure 5, the compound displayed competitive, active-site-directed inhibition because the corresponding IC_{50} values increased linearly with increasing concentration of the reference substrate estriol.

The competitive inhibition constant (K_{ic}) of the secondary sesquiterpenoid alcohol **26b** was determined in order to derive a kinetic parameter that is independent of the substrate concentration. Furthermore, K_{ic} was measured to confirm the high affinity and the mechanism of inhibition displayed by the tricyclic alcohol as indicated by the studies described above. The resulting data were fitted by simultaneous nonlinear regression to the competitive, noncompetitive, mixed-type, and uncompetitive inhibition models, which were ranked according to Akaike's corrected information criterion (results not shown). On the basis of this analysis, the active-site-directed, competitive inhibition model was chosen and the resulting K_{ic} was in good agreement with the expected value, which was calculated from its IC_{50} (Cheng−Prusoff equation; cf. Supporting Information). The very low K_{ic} of 18.4 nM confirmed the high affinity of compound **26b** toward UGT2B7 (Figure 7A).

It was determined that the alcohol **26b** displayed similar affinity levels independent of the substrate used. The substrate independence was assessed by measuring the IC_{50} of the secondary sesquiterpenoid alcohol **26b** toward five different substrates of UGT2B7, namely, 1-naphthol, 4-nitrophenol, scopoletin, epitestosterone, and 4-methylumbelliferone. The measured IC_{50} values ranged from 47 to 79 nM (standard deviation <8.7%, $n = 15$) and confirmed that the high inhibition exerted by **26b** was independent of the substrate employed.

Glucuronidation assays using [^{14}C]UDPGlcA revealed that the secondary alcohol **26b** was not glucuronidated by UGT2B7 at detectable rates and was therefore a true inhibitor of this

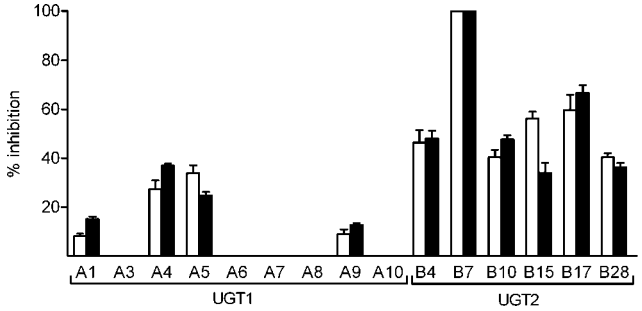

Figure 6. Inhibition of the UGT-catalyzed glucuronidation of umbelliferone and 1-hydroxypyrene by compound **1** (open bars) and inhibitor **26b** (solid bars). Mean values and standard deviations are shown ($n = 4$). The inhibitors were employed at a high concentration of 25 μM, which corresponds to more than 1000K_{ic} for UGT2B7. In addition to UGT2B7, which was completely inhibited, the isoform 2B17 displayed the highest response and was therefore chosen to assess the true selectivity of inhibitor **26b**. The phenyl group had presumably no effect on the isoform selectivity because the percent inhibition exerted by **26b** was similar to that exerted by isolongifolol (**1**).

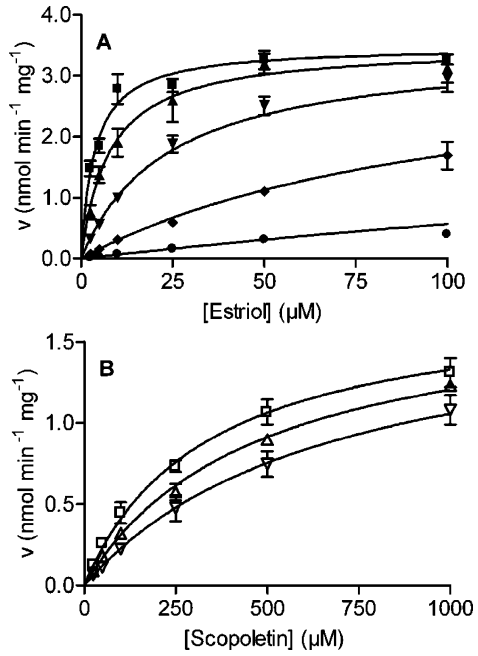

Figure 7. Determination of K_{ic} for inhibitor **26b** assayed with UGT2B7 (A) and UGT2B17 (B). K_{ic} for the UGT2B7-catalyzed estriol glucuronidation was 18.4 nM (standard deviation = 1.51, $n = 90$; $CI_{95\%}$ = 15.3−21.4 nM), which was assayed at inhibitor concentrations of 0.020, 0.10, 0.5, and 2.5 μM. K_{ic} for the UGT2B17-catalyzed scopoletin glucuronidation was 21.8 μM (standard deviation = 1.46, $n = 54$; $CI_{95\%}$ = 18.9−24.7 nM) and was measured at inhibitor concentrations of 10 and 25 μM (inhibitor concentrations >25 μM resulted in solubility problems at high scopoletin concentrations). The true selectivity (K_{ic}^{2B17}/K_{ic}^{2B7}) was >1000; formation of the UGT2B7/**26b** complex was therefore more than 1000-fold favored over formation of the UGT2B17/**26b** complex.

enzyme. The glucuronidation assays were conducted with the enzyme at a high concentration of 2.0 mg of protein mL^{-1} and an incubation time of 16 h in order to identify even small amounts of [^{14}C]β-D-glucuronide. The radioactive labeled co-substrate was used due to the low UV absorption of compound **26b**. The results suggest that steric hindrance in the vicinity of the hydroxy group exerted by the bulky phenyl group prevented enzyme-catalyzed conjugation of the nucleophilic group. Also, other hepatic UGT enzymes did not conjugate the inhibitor because assays with human liver microsomes did not produce the corresponding [^{14}C]β-D-glucuronide. Interestingly, molecular

modeling showed that the phenyl-substituted derivative **26b** was not able to accommodate the GlcA moiety at its hydroxy group due to the steric hindrance exerted by the phenyl group in proximity to the bulky tricyclic scaffold (results not shown).

Isoform selectivity was assessed by measuring the percent inhibition exerted by compound **26b** toward the glucuronidation reaction catalyzed by 14 different recombinant human UGT isoforms of subfamilies 1A and 2B. Umbelliferone and 1-hydroxypyrene were chosen as reference substrates because these compounds are glucuronidated by many different UGT enzymes and can be conveniently analyzed by fluorescence spectroscopy. The inhibitor **26b** was employed at a concentration of 25 μM, which was significantly higher than its K_{ic} for UGT2B7 (>1000-fold). The results indicated that inhibitor **26b** was highly isoform-selective for UGT2B7 (Figure 6). Most of the UGT1A isoforms did not display any significant response to the inhibitor. In contrast, the activity of the UGT2B isoforms was reduced by approximately 30−70% by this high concentration of **26b**. In addition to UGT2B7, which was completely inhibited, the UGT2B17-catalyzed glucuronidation reaction displayed the highest response to the inhibitors (~70% inhibition). Isoform 2B17 was therefore chosen to assess the true selectivity of inhibitor **26b**. The K_{ic} value of **26b** for UGT2B17 was 21.8 μM, and the true selectivity ($K_{ic}^{2B17}/K_{ic}^{2B7}$) of this inhibitor for UGT2B7 was therefore >1000 (Figure 7). The large difference in K_{ic} values was confirmed by measuring the inhibitory activity of **26b** toward the UGT2B7- and UGT2B17-catalyzed glucuronidation of their common substrates 1-naphthol, umbelliferone, and 4-methylumbelliferone (results not shown).

Conclusion

The results of this study indicate that compound **26b** is a highly selective inhibitor for the key enzyme involved in drug glucuronidation, UGT2B7. To our knowledge, no isoform-selective inhibitor for this isoform has been described to date. The preferential inhibition of UGT2B7 is remarkable when the promiscuous character of metabolic enzymes is taken into account. The tricyclo[5.4.0.0^{2,9}]undecane framework is presumably responsible for the high affinity, whereas the phenyl group does not significantly contribute to the inhibition level. The key function of the phenyl group is to increase steric hindrance in the vicinity of the hydroxy group and therefore to decrease the accessibility to this nucleophilic functionality and to prevent enzymatic glucuronidation. The hydroxy group has presumably no significant effect on the formation of the enzyme−inhibitor complex, indicating that there is no significant attractive interaction to the binding site of UGT2B7. The OH group is merely retained to promote the solubility of the compound. Furthermore, the very low K_{ic} of 18 nM is likewise noteworthy since UGTs are commonly described as flexible, promiscuous enzymes that in general do not display low dissociation constants. This nanomolar K_{ic} of the sesquiterpenoid derivative **26b** might indicate specific attractive interactions toward the binding site of UGT2B7. In this respect, it might be suggested that the recognition of small guest molecules is predominantly controlled by mere hydrophobic interactions during the formation of the encounter complex. Hence, the question arises to what extent the UGT enzyme eventually recognizes those chemical groups that serve as nucleophiles in the enzyme-catalyzed reaction.

Experimental Section

Materials. UDPGlcA (trisodium salt, CAS 63700-19-6), saccharic acid-1,4-lactone (CAS 61278-30-6), estriol (CAS 50−27-1), scopoletin (CAS 92-61-5), 4-methylumbelliferone (CAS 90-33-5), and epitestosterone (CAS 481-30-1) were obtained from Sigma (St. Louis, MO). 4-Nitrophenol (CAS 100-02-7), 1-naphthol (CAS 90-15-3), and umbelliferone (CAS 93-35-6) were from Aldrich (Schnelldorf, Germany). Radiolabeled [^{14}C]UDPGlcA was acquired from Perkin-Elmer Life and Analytical Sciences (Boston, MA). HPLC-grade solvents were used throughout the study. The recombinant human UGTs were expressed as His-tagged proteins in baculovirus-infected insect cells as previously described.[47] The cDNA for the human UGT2B17 was a generous gift from Professor Peter Mackenzie (Flinders Medical Centre, Flinders University, Bedford Park, South Australia).

Syntheses. Procedures for the syntheses and characterization of the compounds are given in the Supporting Information.

X-ray Crystal Structures. Crystallographic data for the X-ray measurements of **12b**, **14a**, **16a**, **17a**, **19b**, **20a**, **21b**, and **22a** are given in the Supporting Information. Crystal data were collected on an Oxford Gemini S diffractometer (Cu-K_α radiation, λ = 1.542 48 Å, for **12b**, **16a**, **17a**, **19b**, **20a**, **21b**, and **22a**; Mo-K_α radiation, λ = 0.710 73 Å, for **14a**) at 100 K. All structures were solved by direct methods (SHELXS-97)[49] and refined by full-matrix least-squares methods against F^2 (SHELXL-97).[50] All non-hydrogen atoms were refined anisotropically. All hydrogen atom positions, except O-bonded hydrogen atoms, were refined by use of a riding model. The positions of O-bonded hydrogen atoms were taken from the difference Fourier map and refined isotropically. The absolute structures were determined with respect to the Flack parameter.[51]

In **19b**, the chlorine atoms of the two crystallographic independent molecules (**19ba** and **19bb**) are disordered and were refined on two positions. Occupation factors were determined as follows: **19ba** (Cl1 = 0.531; Cl1A = 0.469) and **19bb** (Cl2 = 0.484; Cl2A = 0.516).

In **22a**, the =CH_2 group of one of the two crystallographic independent molecules is disordered and was refined disordered on two positions. Occupation factors were determined as follows: C18 = 0.442 and C18A = 0.558.

CCDC-623771 (**12b**), CCDC-623772 (**14a**), CCDC-623773 (**16a**), CCDC-623774 (**17a**), CCDC-623775 (**19b**), CCDC-623776 (**20a**), CCDC-623777 (**21b**), CCDC-623778 (**22a**), CCDC-623779 [(*E*)-**33**], and CCDC-623780 [(*Z*)-**3**] contain the supplementary crystallographic data. These data can be obtained free of charge from The Cambridge Crystallographic Data Centre via www.ccdc.cam.ac.uk/data_request/cif.

Inhibitor Screening. Percent inhibition was measured at four inhibitor concentrations (0.10, 1.0, 10, and 100 μM) with estriol as the reference substrate (25 μM). The reaction mixture consisted of phosphate buffer (50 mM, pH 7.4), $MgCl_2$ (10 mM), and saccharic acid-1,4-lactone (5.0 mM). The concentration of UGT2B7 was 0.10 mg of protein mL^{-1}. Assays in the absence of inhibitor, blank runs in the absence of cosubstrate, and control assays employing isolongifolol were included in each assay. The enzyme reaction was initiated by the addition of a solution of UDPGlcA to a final concentration of 5.0 mM. The enzyme reactions were terminated after an incubation time of 15 min at 37 °C by the addition of ice-cold perchloric acid (4.0 M) and transfer to ice. The mixtures were centrifuged (16000*g*, 10 min) and aliquots of the supernatants were subjected to HPLC analysis. Results reflect a minimum of three replicate determinations.

IC_{50} Values. The IC_{50} values of compound **26b** were determined at five concentrations bracketing its apparent IC_{50} (0.10, 0.25, 1.0, 4.0, and 10 × IC_{50}). Estriol was employed at six [S]/K_m ratios (0.5, 1.0, 2.0, 5.0, 10, and 20). The reaction mixture consisted of phosphate buffer (50 mM, pH 7.4), $MgCl_2$ (10 mM), and saccharic acid-1,4-lactone (5.0 mM). The enzyme UGT2B7 was employed at 0.10 mg of protein mL^{-1}. Assays in the absence of inhibitor, blank runs in the absence of cosubstrate, and control assays with isolongifolol at a fixed concentration of 0.10 μM were included at each [S]/K_m ratio. The enzyme reaction was initiated after a 5 min preincubation time at 37 °C by addition of a solution of UDPGlcA to a final concentration of 5.0 mM. Enzyme reactions were terminated after an incubation time of 15 min at 37 °C by the addition of ice-cold perchloric acid (4.0 M) and transfer to ice.

The mixtures were centrifuged (16000*g*, 10 min) and aliquots of the supernatants were subjected to HPLC analysis. The data were analyzed by nonlinear regression with the two-parameter Hill equation. Results reflect a minimum of three replicate determinations.

Testing for Reversibility. UGT2B7 at a concentration of 5.0 mg of protein mL^{-1} was preincubated in buffered solution (phosphate buffer, 50 mM, pH 7.4) at 37 °C with a concentration of **26b** equivalent to 10 times its IC_{50}. After an equilibration time of 45 min, this mixture was diluted 50-fold into reaction buffer (37 °C) containing the reference substrate estriol (25 μM), phosphate buffer (50 mM, pH 7.4), UDPGlcA (5.0 mM), $MgCl_2$ (10 mM), and saccharic acid-1,4-lactone (5.0 mM) to initiate reaction. The formation of glucuronide was monitored every 2.5 min over 60 min by pipetting 100 μL of the reaction buffer to a vial containing 10 μL of perchloric acid (4.0 M). The acidified mixtures were transferred to ice and centrifuged (16000*g*, 10 min), and aliquots of the supernatants were subjected to HPLC analysis. Control assays in the absence of terpenoid alcohol were included. Results reflect a minimum of two replicate determinations (Supporting Information).

Inhibitory Dissociation Constants. The K_{ic} value for UGT2B7 (0.10 mg of protein mL^{-1}) was determined at six estriol concentrations (2.5, 5.0, 10, 25, 50, and 100 μM), and the inhibitor **26b** was employed at four concentrations (0.020, 0.10, 0.50, and 2.5 μM). The K_{ic} value for UGT2B17 (0.15 mg protein mL^{-1}) was measured at six scopoletin concentrations (25, 50, 100, 250, 500, and 1000 μM), and compound **26b** was used at two concentrations of 10 and 25 μM. For estriol assays: Enzyme reactions were initiated after a 5.0 min preincubation at 37 °C by addition of a solution of UDPGlcA to a final concentration of 5.0 mM. Enzyme reactions were terminated after 15 min at 37 °C by addition of ice-cold perchloric acid (4.0 M) and transfer to ice. The mixtures were centrifuged (16000*g*, 10 min), and aliquots of the supernatants were subjected to HPLC analysis. Results reflect a minimum of three replicate determinations. For scopoletin assays: Enzyme reactions were initiated after a 5 min preincubation at 37 °C by addition of a solution of UDPGlcA to a final concentration of 5.0 mM. Enzyme reactions were terminated after 10 min at 37 °C by addition of ice-cold perchloric acid (4.0 M) and transfer to ice. The mixtures were centrifuged (16000*g*, 10 min), and aliquots of the supernatants were subjected to HPLC analysis. Results reflect a minimum of three replicate determinations.

Testing for Substrate-Independent Inhibition. IC_{50} values of inhibitor **26b** were determined by use of five different reference substrates. Assay conditions were balanced with the substrates at concentrations that resembled their K_m values for UGT2B7: 1-naphthol (300 μM, 0.20 mg of protein mL^{-1}, incubation time 20 min), 4-nitrophenol (500 μM, 0.10 mg of protein mL^{-1}, incubation time 10 min), scopoletin (320 μM, 0.10 mg of protein mL^{-1}, incubation time 10 min), epitestosterone (15 μM, 0.25 mg of protein mL^{-1}, incubation time 20 min), and 4-methylumbelliferone (600 μM, 0.20 mg of protein mL^{-1}, incubation time 20 min). Compound **26b** was employed at five concentrations bracketing its IC_{50} (0.10, 0.25, 1.0, 4.0, and 10 × IC_{50}). Assays were carried out as described above. Results reflect a minimum of two replicate determinations.

Isoform Selectivity. Umbelliferone (100 μM) was used as substrate for UGT isoforms 1A1 (0.15 mg of protein mL^{-1}), 1A7 (0.15 mg of protein mL^{-1}), 1A8 (0.11 mg of protein mL^{-1}), 1A9 (0.15 mg of protein mL^{-1}), 1A10 (0.12 mg of protein mL^{-1}), and 2B7 (0.10 mg of protein mL^{-1}). UGTs 1A3 (0.40 mg of protein mL^{-1}), 1A4 (0.50 mg of protein mL^{-1}), 1A5 (0.11 mg of protein mL^{-1}), 1A6 (0.10 mg of protein mL^{-1}), 2B4 (0.50 mg of protein mL^{-1}), 2B10 (0.26 mg of protein mL^{-1}), 2B15 (0.50 mg of protein mL^{-1}), 2B17 (0.20 mg of protein mL^{-1}), and 2B28 (0.25 mg of protein mL^{-1}) were assayed with 1-hydroxypyrene (50 μM). Isolongifolol (**1**) and inhibitor **26b** were employed at concentrations of 10, 25, and 50 μM. Enzyme reactions were initiated after 5 min preincubation at 37 °C by addition of a solution of UDPGlcA to a final concentration of 5.0 mM. For umbelliferone assays: Enzyme reactions were terminated after 25 min at 37 °C by addition of ice-cold perchloric acid (4.0 M) and transfer to ice. The mixtures were centrifuged (16000 *g*, 10 min), and aliquots of the supernatants were subjected to HPLC analysis. For 1-hydroxypyrene assays: Enzyme reactions were terminated after 20 min at 37 °C by addition of ice-cold aqueous $ZnSO_4$ (15% by weight), followed by acetonitrile, and transfer to ice. The mixtures were centrifuged (16000*g*, 10 min), and aliquots of the supernatants were subjected to HPLC analysis. Results reflect a minimum of four replicate determinations.

Glucuronidation Assays. Formation of glucuronide was assayed by use of radiolabeled [^{14}C]UDPGlcA.[48] A solution of [^{14}C]-UDPGlcA (400 μL, 196 mCi $mmol^{-1}$, 0.02 mCi mL^{-1} in EtOH/water, 7:1 v/v) was transferred to 2-mL vials and the solvent was evaporated in vacuo at room temperature. The residue was dissolved in reaction buffer (90 μL), which consisted of either UGT2B7 (2.0 mg of protein mL^{-1}) or human liver microsomes (100 μg), $MgCl_2$ (10 mM), phosphate buffer (50 mM, pH 7.4), and saccharic acid-1,4-lactone (5.0 mM). A solution of inhibitor **26b** (1.0 mM in 50 vol % DMSO/water) was added to the reaction buffer to a final saturating concentration of 100 μM (approximately $5500K_{ic}^{2B7}$). After incubation for 16 h at 37 °C, the reaction mixture was centrifuged (16000 *g*, 10 min), and aliquots of the supernatants were subjected to HPLC analysis. Control assays in the presence of the substrate isolongifolol (100 μM) and blank runs were included. The detection limit (25 pmol, signal-to-noise ratio = 10:1) was determined by subjecting dilutions of reaction buffer containing isolongifolol [^{14}C]β-D-glucuronide to HPLC analysis. Results reflect a minimum of two replicate determinations.

HPLC Methods. The HPLC system consisted of the Agilent 1100 series degasser, binary pump, autosampler, thermostated column compartment, multiple wavelength detector, and fluorescence detector (Agilent Technologies, Palo Alto, CA). The resulting spectra were analyzed with Agilent ChemStation software (rev. B.01.01). Glucuronidation reaction products were separated and detected as follows. Estriol β-D-glucuronide: Hypersil BDS-C18 (150 × 4.6 mm; Agilent Technologies, Palo Alto, CA); 35% MeOH in phosphate buffer (50 mM, pH 3.0); flow rate 1.0 mL min^{-1}; detection by fluorescence spectroscopy (excitation at λ 335 nm, emission at λ 455 nm); retention time 4.2 min. 4-Nitrophenol β-D-glucuronide: Chromolith SpeedROD (50 × 4.6 mm; Merck, Darmstadt, Germany); 15% acetonitrile in phosphate buffer (50 mM, pH 3.0); flow rate 1.0 mL min^{-1}; detection by UV spectroscopy (λ 300 nm); retention time 1.3 min. Scopoletin β-D-glucuronide: Chromolith SpeedROD (50 × 4.6 mm); 10% MeOH in phosphate buffer (50 mM, pH 3.0); flow rate (gradient run) 0.8 mL min^{-1} (0.0−4.5 min), 0.8 mL → 2.5 mL min^{-1} (4.5−5.0 min), 2.5 mL min^{-1} (5.0−11.0 min), 2.5 → 0.8 mL min^{-1} (11.0−12 min); detection by fluorescence spectroscopy (excitation at λ 335 nm, emission at λ 455 nm); retention time 4.2 min. Epitestosterone β-D-glucuronide: Chromolith SpeedROD (50 × 4.6 mm); 43% MeOH in phosphate buffer (50 mM, pH 3.0); flow rate 2.0 mL min^{-1}; detection by UV spectroscopy (λ 246 nm); retention time 5.9 min. 1-Naphthol β-D-glucuronide: Hypersil BDS-C18 (150 × 4.6 mm); 42% MeOH in phosphate buffer (50 mM, pH 3.0); flow rate 1.0 mL min^{-1}; detection by fluorescence spectroscopy (excitation at λ 285 nm, emission at λ 335 nm); retention time 4.9 min. Umbelliferone β-D-glucuronide: Chromolith SpeedROD (50 × 4.6 mm); 15% MeOH in phosphate buffer (50 mM, pH 3.0); flow rate 1.5 mL min^{-1}; detection by fluorescence spectroscopy (excitation at λ 316 nm, emission at λ 382 nm); retention time 1.4 min. 4-Methylumbelliferone β-D-glucuronide: Chromolith SpeedROD (50 × 4.6 mm); 20% MeOH in phosphate buffer (50 mM, pH 3.0); flow rate 2.0 mL min^{-1}; detection by fluorescence spectroscopy (excitation at λ 316 nm, emission at λ 382 nm); retention time 1.3 min. 1-Hydroxypyrene β-D-glucuronide: Hypersil BDS-C18 (150 × 4.6 mm); 40% acetic acid (0.5 vol %) in acetonitrile; flow rate 0.9 mL min^{-1}; detection by fluorescence spectroscopy (excitation at λ 237 nm, emission at λ 388 nm); retention time 2.3 min. [^{14}C]β-D-Glucuronides: Chromolith SpeedROD (50 × 4.6 mm); gradient run 5% MeOH in phosphate buffer (50 mM, pH 3.0; 0.0−3.5 min), 5% → 80% MeOH (3.5−8.0 min), 80% MeOH (8.0−13 min), 80% → 5% MeOH (13−15 min), 5% MeOH (15−20 min); flow rate

1.0 mL min^{-1}; retention time for isolongifolol [^{14}C]β-D-glucuronide 9.3 min; detection by use of a 9701 HPLC radioactivity monitor (Reeve Analytical, Glasgow, Scotland).

Acknowledgment. We thank Sanna Sistonen for conducting some of the isoform-selectivity assays, Olli Aitio for his help with the gNOESY experiments, and Sirkku Jäntti for conducting the LC-MS analyses. This work was supported by a fellowship from the Finnish Cultural Foundation (IB), a grant from Walter och Lisi Wahls Stiftelse för Naturvetenskaplig Forskning, and the Academy of Finland (Projects 207535 and 210933).

Supporting Information Available: Degree of purity (elemental analysis), synthesis procedures, spectroscopic data, X-ray crystal structures, ^{1}H−^{13}C correlation data, gHSQC and ^{13}C NMR spectra, and testing for reversibility of inhibition. This material is available free of charge via the Internet at http://pubs.acs.org.

References

(1) Radominska-Pandya, A.; Ouzzine, M.; Fournel-Gigleux, S.; Magdalou, J. Structure of UDP-glucuronosyltransferases in membranes. *Methods Enzymol.* **2005**, *400*, 116−147.
(2) Wells, P. G.; Mackenzie, P. I.; Chowdhury, J. R.; Guillemette, C.; Gregory, P. A.; Ishii, Y.; Hansen, A. J.; Kessler, F. K.; Kim, P. M.; Chowdhury, N. R.; Ritter, J. K. Glucuronidation and the UDP-glucuronosyltransferases in health and disease. *Drug Metab. Dispos.* **2004**, *32*, 281−290.
(3) Fisher, M. B.; Paine, M. F.; Strelevitz, T. J.; Wrighton, S. A. The role of hepatic and extrahepatic UDP-glucuronosyltransferases in human drug metabolism. *Drug Metab. Rev.* **2001**, *33*, 273−297.
(4) Owens, I. S.; Basu, N. K.; Banerjee, R. UDP-glucuronosyltransferases: gene structures of UGT1 and UGT2 families. *Methods Enzymol.* **2005**, *400*, 1−22.
(5) Williams, J. A.; Hyland, R.; Jones, B. C.; Smith, D. A.; Hurst, S.; Goosen, T. C.; Peterkin, V.; Koup, J.; Ball, S. E. Drug−drug interactions for UDP-glucuronosyltransferase substrates: a pharmacokinetic explanation for typically observed low exposure (AUCi/AUC) ratios. *Drug Metab. Dispos.* **2004**, *32*, 1201−1208.
(6) The term catalytic promiscuity has been used to describe the ability of an enzyme to catalyze an adventitious secondary activity at the active site responsible for the primary activity. However, in the case of metabolic enzymes like UGTs, the term has been used to depict their overlapping substrate selectivities. Cf. Copley, S. D. Enzymes with extra talents: moonlighting functions and catalytic promiscuity. *Curr. Opin. Chem. Biol.* **2003**, *7*, 265−272.
(7) Court, M. H. Isoform-selective probe substrates for in vitro studies of human UDP-glucuronosyltransferases. *Methods Enzymol.* **2005**, *400*, 104−116.
(8) Lightstone, F. C.; Ya-Jun, Z.; Maulitz, A. H.; Bruice, T. C. Nonenzymatic and enzymatic hydrolysis of alkyl halides: a haloalkane dehalogenation enzyme evolved to stabilize the gas-phase transition state of an S_N2 displacement reaction. *Proc. Natl. Acad. Sci. U.S.A.* **1997**, *94*, 8417−8420.
(9) Markham, G. D.; Parkin, D. W.; Mentch, F.; Schramm, V. L. A kinetic isotope effect study and transition state analysis of the *S*-adenosylmethionine synthetase reaction. *J. Biol. Chem.* **1987**, *262*, 5609−5615.
(10) Schramm, V. L. Enzymatic transition states: thermodynamics, dynamics and analogue design. *Arch. Biochem. Biophys.* **2005**, *433*, 13−26.
(11) Taylor Ringia, E. A.; Schramm, V. L. Transition states and inhibitors of the purine nucleoside phosphorylase family. *Curr. Top. Med. Chem.* **2005**, *5*, 1237−1258.
(12) Grancharov, K.; Naydenova, Z.; Lozeva, S.; Golovinsky, E. Natural and synthetic inhibitors of UDP-glucuronosyltransferase. *Pharmacol. Ther.* **2001**, *89*, 171−186.
(13) Timmers, C. M.; Dekker, M.; Buijsman, R. C.; van der Marel, G. A.; Ethell, B.; Anderson, G.; Burchell, B.; Mulder, G. J.; van Boom, J. H. Synthesis and inhibitory effect of a trisubstrate transition state analog for UDP glucuronosyltransferases. *Bioorg. Med. Chem. Lett.* **1997**, *7*, 1501−1506.
(14) Noort, D.; Meijer, E. A.; Visser, T. J.; Meerman, J. H. N.; van der Marel, G. A.; van Boom, J. H.; Mulder, G. J. Selective inhibition of glucuronidation by 2,2,2-triphenylethyl-UDP in isolated rat hepatocytes: conjugation of harmol, 3,3′,5-triiodothyronine, and *N*-hydroxy-2-acetylaminofluorene. *Mol. Pharmacol.* **1991**, *40*, 316−320.
(15) Schramm, V. L. Enzymatic transition states and transition state analogues. *Curr. Opin. Struct. Biol.* **2005**, *15*, 604−613.
(16) Schramm, V. L. Enzymatic transition states and transition state analog design. *Annu. Rev. Biochem.* **1998**, *67*, 693−720.
(17) Said, M.; Noort, D.; Magdalou, J.; Ziegler, J. C.; van der Marel, G. A.; van Boom, J. H.; Mulder, G. J.; Siest, G. Selective and potent inhibition of different hepatic UDP-glucuronosyltransferase activities by ω,ω,ω-triphenylalcohols and UDP derivatives. *Biochem. Biophys. Res. Commun.* **1992**, *187*, 140−145.
(18) Noort, D.; Coughtrie, M. W.; Burchell, B.; van der Marel, G. A.; van Boom, J. H.; van der Gen, A.; Mulder, G. J. Inhibition of UDP-glucuronosyltransferase activity by possible transition-state analogues in rat-liver microsomes. *Eur. J. Biochem.* **1990**, *188*, 309−312.
(19) Uchaipichat, V.; Mackenzie, P. I.; Elliot, D. J.; Miners, J. O. Selectivity of substrate (trifluoperazine) and inhibitor (amitriptyline, androsterone, canrenoic acid, hecogenin, phenylbutazone, quinidine, quinine, and sulfinpyrazone) "probes" for human UDP-glucuronosyltransferases. *Drug Metab. Dispos.* **2006**, *34*, 449−456.
(20) Sell, C. S. *A fragrant introduction to terpenoid chemistry*; The Royal Society of Chemistry: Cambridge, U.K., 2003; pp 203−214.
(21) Corey, E. J.; Ohno, M.; Vatakencherry, P. A.; Mitra, R. B. Total synthesis of D,L-longifolene. *J. Am. Chem. Soc.* **1961**, *83*, 1251−1253.
(22) Volkmann, R. A.; Andrews, G. C.; Johnson, W. S. Novel synthesis of longifolene. *J. Am. Chem. Soc.* **1975**, *97*, 4777−4779.
(23) Schultz, A. G.; Puig, S. The intramolecular diene−carbene cycloaddition equivalence and an enantioselective Birch reduction−alkylation by the chiral auxiliary approach. Total synthesis of (±)-and (−)-longifolene. *J. Org. Chem.* **1985**, *50*, 915−916.
(24) Jadhav, P. K.; Brown, H. C. Dilongifolylborane: a new effective chiral hydroborating agent with intermediate steric requirements. *J. Org. Chem.* **1981**, *46*, 2988−2990.
(25) Dimitrov, V.; Linden, A.; Hesse, M. Chiral ferrocenes derived from (+)-longifolene−determination of the configuration by NMR spectroscopy and X-ray crystallography. *Tetrahedron: Asymmetry* **2001**, *12*, 1331−1335.
(26) Arigoni, D. Stereochemical aspects of sesquiterpene biosynthesis. *Pure Appl. Chem.* **1975**, *41*, 219−245.
(27) Yoshikuni, Y.; Ferrin, T. E.; Keasling, J. D. Designed divergent evolution of enzyme function. *Nature* **2006**, *440*, 1078−1082.
(28) Koistinen, J.; Lehtonen, M.; Tukia, K.; Soimasuo, M.; Lahtiperä, M.; Oikari, A. Identification of lipophilic pollutants discharged from a Finnish pulp and paper mill. *Chemosphere* **1998**, *37*, 219−235.
(29) Passino-Reader, D. R.; Hickey, J. P.; Ogilvie, L. M. Toxicity to *Daphnia pulex* and QSAR predictions for polycyclic hydrocarbons representative of Great Lakes contaminants. *Bull. Environ. Contam. Toxicol.* **1997**, *59*, 834−840.
(30) Ishida, T.; Asakawa, Y.; Takemoto, T. Hydroxyisolongifolaldehyde: a new metabolite of (+)-longifolene in rabbits. *J. Pharm. Sci.* **1982**, *71*, 965−966.
(31) Rubio, J.; Calderon, J. S.; Flores, A.; Castroa, C. Trypanocidal activity of oleoresin and terpenoids isolated from *Pinus oocarpa*. *Z. Naturforsch. C* **2005**, *60*, 711−716.
(32) Sawaikar, D. D.; Sinha, B.; Hebbalkar, G. D.; Sharma, R. N.; Patwardhan, S. A. Products active on mosquitoes. Part VII. Synthesis and biological activity of longifolene derivatives. *Indian J. Chem. B* **1995**, *34*, 832−835.
(33) Choudhary, M. I.; Musharraf, S. G.; Nawaz, S. A.; Anjum, S.; Parvez, M.; Fun, H.-K.; Atta-ur-Rahman. Microbial transformation of (−)-isolongifolol and butyrylcholinesterase inhibitory activity of transformed products. *Bioorg. Med. Chem. Lett.* **2005**, *13*, 1939−1944.
(34) Bichlmaier, I.; Siiskonen, A.; Finel, M.; Yli-Kauhaluoma, J. Stereochemical sensitivity of the human UDP-glucuronosyltransferases 2B7 and 2B17. *J. Med. Chem.* **2006**, *49*, 1818−1827.
(35) Bichlmaier, I.; Siiskonen, A.; Kurkela, M.; Finel, M.; Yli-Kauhaluoma, J. Chiral distinction between the enantiomers of bicyclic alcohols by UDP-glucuronosyltransferases 2B7 and 2B17. *Biol. Chem.* **2006**, *387*, 407−416.
(36) Bichlmaier, I.; Kurkela, M.; Siiskonen, A.; Finel, M.; Yli-Kauhaluoma, J. Eudismic analysis of tricyclic sesquiterpenoid alcohols. Lead structures for the design of potent inhibitors of the human UDP-glucuronosyltransferase 2B7. *Bioorg. Chem.* (submitted).
(37) Ladziata, U.; Zhdankin, V. V. Hypervalent iodine(V) reagents in organic synthesis. *ARKIVOC: Arch. Org. Chem.* **2006**, *ix*, 26−58.
(38) Frigerio, M.; Santagostino, M.; Sputore, S. A user friendly entry to 2-iodoxybenzoic acid (IBX). *J. Org. Chem.* **1999**, *64*, 4537−4538.
(39) Mizuta, T.; Sakaguchi, S.; Ishii, Y. Catalytic reductive alkylation of secondary amine with aldehyde and silane by an iridium compound. *J. Org. Chem.* **2005**, *70*, 2195−2199.
(40) Concellón, J. M.; Cuervo, H.; Férnandez-Fano, R. An improved preparation of epoxides from carbonyl compounds by using diiodomethane/methyllithium: synthetic applications. *Tetrahedron* **2001**, *57*, 8983−8987.
(41) Li, Z.; Racha, S; Dan, L.; El-Subbagh, H.; Abushanab, E. A general and facile synthesis of β- and γ-hydroxyphosphonates from epoxides. *J. Org. Chem.* **1993**, *58*, 5779−5783.

(42) Samadder, P.; Bittman, R.; Byun, H.-S.; Arthur, G. Synthesis and use of novel ether phospholipid enantiomers to probe the molecular basis of the antitumor effects of alkyllysophospholipids: Correlation of differential activation of c-Jun NH_2-terminal protein kinase with antiproliferative effects in neuronal tumor cells. *J. Med. Chem.* **2004**, *47*, 2710−2713.
(43) Chandran, S. S.; Frost, J. W. Aromatic inhibitors of dehydroquinate synthase: Synthesis, evaluation and implications for gallic acid biosynthesis. *Bioorg. Med. Chem. Lett.* **2001**, *11*, 1493−1496.
(44) Parrish, J. D.; Shelton, D. R.; Little, R. D. Titanocene(III)-promoted Reformatsky additions. *Org. Lett.* **2003**, *5*, 3615−3617.
(45) Alternatively, gNOESY experiments could be used for the assignment of the absolute configuration at C(1′). The NOE correlation between C(1′)O*H* and *endo*-C(10)*H* was present when the OH group was pointing toward *endo*-C(10)*H*. In contrast, this NOE correlation was not found in its corresponding epimer in which the OH group was pointing away from *endo*-C(10)*H*. However, these correlations were often difficult to assign due to signal overlap, and, therefore, gHSQC analysis was superior because all corresponding signals were resolved.
(46) Copeland, R. A. *Evaluation of enzyme inhibitors in drug discovery*; John Wiley & Sons: Hoboken, NJ, 2005.
(47) Kurkela, M.; Garcia-Horsman, A.; Luukkanen, L.; Mörsky, S.; Taskinen, J.; Baumann, M.; Kostiainen, R.; Hirvonen, J.; Finel, M. Expression and characterization of recombinant human UDP-glucuronosyltransferases (UGTs). UGT1A9 is more resistant to detergent inhibition than other UGTs and was purified as an active dimeric enzyme. *J. Biol. Chem.* **2003**, *278*, 3536−3544.
(48) Kaivosaari, S.; Salonen, J. S.; Mortensen, J.; Taskinen, J. High-performance liquid chromatographic method combining radiochemical and ultraviolet detection for determination of low activities of uridine 5′-diphosphate-glucuronosyltransferase. *Anal. Biochem.* **2001**, *292*, 178−187.
(49) Sheldrick, G. M. Phase annealing in SHELX-90: direct methods for larger structures. *Acta Crystallogr., Sect. A* **1990**, *46*, 467−473.
(50) Sheldrick, G. M. *SHELXL-97, A program for crystal structure refinement*; Göttingen, Germany, 1996.
(51) Flack, H. D. On enantiomorph-polarity estimation. *Acta Crystallogr., Sect. A* **1983**, *39*, 876−881.

JM061204E